

PHYSICAL AND ANALYTICAL CHEMISTRY

Article

Received: 22 January 2024 | Revised: 27 March 2024 |
Accepted: 9 April 2024 | Published online: 24 April 2024

UDC 544.42+519.242.7

<https://doi.org/10.31489/2959-0663/2-24-13>

Alexander L. Kwiatkowski^{1*} , Vyacheslav S. Molchanov¹ , Anton S. Orekhov² ,
Alexander I. Kuklin³ , Olga E. Philippova¹ 

¹Physics Department, Lomonosov Moscow State University, Moscow, Russia;

²National Research Center, Kurchatov Institute, Moscow, Russia;

³Joint Institute for Nuclear Research, Dubna, Russia

(*Corresponding author's e-mail: kvyatkovskij@physics.msu.ru)

Detecting Shape of Hybrid Polymer/Surfactant Micelles: Cryo-Transmission Electron Microscopy, Small-Angle Neutron Scattering and Dynamic Light Scattering Study

In-depth study of shape of hybrid micelles in the micellar solutions of anionic surfactant potassium oleate, containing hydrophobic polymer poly(4-vinylpyridine) (P4VP) was conducted via cryo-transmission electron microscopy (cryo-TEM), small-angle neutron scattering (SANS) and dynamic-light scattering of visible light (DLS). Direct visualization of the solutions with cryo-TEM evidenced the coexistence of polymer-free spherical micelles and branched rodlike hybrid micelles with mean length of 200 nm and radius of 2 nm, governed by contour length of solubilized P4VP and length of hydrophobic “tail” of potassium oleate, respectively. The formation of branches in the hybrid micelles was explained by attaching the thermodynamically unfavorable end-caps of micelles to their polymer-loaded cylindrical fragments. By SANS it was shown that the cylindrical local shape and the radius of the micelles are independent of the concentration of embedded P4VP. Relaxation processes in the solutions were investigated with DLS. Three relaxation modes were observed for hybrid micelles, similar to polymer-free wormlike micelles. Fast and medium relaxation modes were attributed to diffusion of entangled micellar chains and their segments, respectively. The slow mode was related to electrostatic repulsion between similarly charged hybrid micelles.

Keywords: ionic surfactant, polymer-surfactant interactions, rodlike micelles, hybrid micelles, branching points, cryo-TEM, SANS, DLS.

Introduction

Self-organization of surfactants into the micelles of different shapes is of extensive attention of scientists during the last three decades [1–4]. Hydrophobic attraction of “tails” and electrostatic repulsion of charged hydrophilic “heads” of ionic surfactants define the shape of the resulting aggregate [2, 5]. Wormlike micelles (WLMs) are aggregates of cylindrical form that consist of two hemispheric end-caps and central cylindrical part [3, 6–8]. Examples of practical applications of semi-dilute solutions of WLMs include their use as foaming agents [9], thickeners for fracturing fluids and cosmetic products [3, 7], drag-reducers [10–11] and drug delivery systems [12, 13].

Incorporation of a polymer into the WLMs of a surfactant results in the formation of hybrid micelles [14–20] that possess the unique properties of both components. For example, recently obtained hybrid micelles of anionic surfactant potassium oleate with embedded hydrophobic polymer poly(4-vinylpyridine) (P4VP) demonstrated both high response to hydrocarbon inherent to surfactant-based fracturing fluid and enhanced drag reducing efficiency inherent to polymer chains [21]. Thus, semi-dilute solution

of the hybrid micelles could potentially be used not only as a fracturing fluid in oil production, but also as a drag-reducer for oil transportation.

In the previous papers [20–22], solutions of the hybrid micelles, saturated with P4VP, were investigated. Since the incorporated polymer influences the hydrophilic-hydrophobic balance of the micelles [20], the concentration of solubilized P4VP is the key parameter that governs their shape. The current paper is devoted to the detailed experimental study of the shape of the hybrid micelles, containing different amount of P4VP. Cryo-transmission electron microscopy (cryo-TEM) was used to directly image the micelles, while contrast matching technique in small-angle neutron scattering (SANS) was employed to investigate their local shape. Additionally, dynamic light scattering of visible light (DLS) provided information about relaxation processes in their aqueous solutions.

Experimental

Materials. Anionic surfactant potassium oleate (purity >98 %) from TCI Europe, inorganic salt KCl (purity > 99.5 %) from Fluka, ethanol (purity > 99 %) from Merck, KOH (purity > 99 %) from Acros Organics, and polymer P4VP (molar mass 60000 g/mol, contour length 140 nm) from Sigma-Aldrich were used as received. Water was purified using a Millipore Milli-Q system. For SANS experiments, mixture of water and deuterium oxide (purity 99.9 %, Sigma-Aldrich) was used as a solvent.

Sample preparation. Stock solutions of polymer-free WLMs were obtained by mixing 47 mM potassium oleate and 80 mM KCl with Milli-Q water and stirred with a magnetic stirrer for 24 hours. The pH of the solutions was kept at 11 with aqueous solution of 1 M KOH. Under these conditions the WLMs were formed in the samples [22].

Hybrid micelles were prepared by pouring the micellar stock solution on the thin polymer film. The film was prepared by full evaporation of ethanol from the drop of 5 wt.% P4VP solution in ethanol on the bottom of vial at room temperature. P4VP embedded into the micelles after stirring the stock solution of polymer-free micelles in the vial with polymer film using magnetic stirrer for 1 day. Content of P4VP in the final solutions was varied from 0.01 to 0.04 monomol/L (amount of monomer units per 1 L of solution).

Cryogenic transmission electron microscopy (cryo-TEM). Cryo-TEM experiments were performed using a Titan Krios (Thermo Fisher Scientific, Hillsboro, OR, USA) at acceleration voltage of 300 kV in bright-field TEM in a low-dose imaging mode. The microscope was equipped with a Falcon 2 direct electron detector (Thermo Fisher Scientific, Hillsboro, OR, USA). To receive the clear images of the aggregates, the stock solution of 47 mM potassium oleate and 0.02 monomol/L P4VP was diluted 4 times with aqueous solution containing 80 mM KCl. The samples were applied onto the Lacey carbon-coated side of the 300 mesh copper TEM grid with Vitrobot Mark 4 (Thermo Fisher Scientific, Hillsboro, OR, USA) [23]. After blotting the excess of the solution with filter paper the grid was plunged into liquid ethane. The images were processed with EPU 3.6 software.

Small-angle neutron scattering (SANS). SANS measurements were carried out using time-of-flight spectrometer YuMO of high-flux pulsed reactor IBR-2M (Joint Institute for Nuclear Research, Dubna, Russia). Details of the experiments and data treatment are described elsewhere [24]. The values of scattering length densities for potassium oleate, monomer unit of P4VP and deuterium oxide, calculated with SasView-5.0 program (<http://www.sasview.org/>), equaled to $\rho_{OK} = 0.15 \cdot 10^{-6} \text{ \AA}^{-2}$, $\rho_{P4VP} = 2.00 \cdot 10^{-6} \text{ \AA}^{-2}$ and $\rho_{D2O} = 6.38 \cdot 10^{-6} \text{ \AA}^{-2}$, respectively. To obtain scattering from potassium oleate molecules in the hybrid micelles, the contrast variation technique was applied. The mixture of deuterium oxide and water with volume ratio $D_2O/H_2O=37/73$ (v/v) was used as a solvent in the experiments to match the scattering from P4VP. The samples were put into the Hellma quartz cuvettes of 1 mm width. Temperature was kept at 20 °C. Data was obtained in the scattering vectors Q range from $6 \cdot 10^{-3}$ to $6 \cdot 10^{-1} \text{ \AA}^{-1}$.

Dynamic-light scattering of visible light (DLS). DLS data were collected with ALV/DLS/SLS-5022F (ALV GmbH, Langen, Germany). Scattering intensity was analyzed with ALV6010/EPP digital correlator. Variation of scattering angle was made by stepping-motor-driven goniometer system. Helium–neon laser (wavelength of 632.8 nm) was used as a light source. The temperature of the samples was kept at 20 °C by a thermostat Lauda Ecoline RE 306. The samples were filtered through 0.45 μm filter (Millipore Millex-FG) to prevent the intrusion of dust. Contin method was applied for data treatment [25].

Results and Discussion

The solutions of potassium oleate with embedded P4VP macromolecules were visualized by cryo-TEM (Fig. 1). In Figure 1 coexisting spherical and rodlike aggregates with mean length of 200 nm can be

observed. The mean radii of cross section spherical and rodlike aggregates are circa equal to 2 nm and coincide with the length of the alkyl “tail” of potassium oleate [22]. Consequently, the observed spherical aggregates are, probably, polymer-free micelles of potassium oleate. The estimated mean length of the rodlike micelles (Fig. 1) is close to the contour length of P4VP. One can also easily detect many “Y-shaped” branching points in the rodlike micelles (Fig. 1). Note that zero-shear viscosity of the polymer-free micellar solution, containing similar amount of potassium oleate and KCl, as was demonstrated by steady shear rheological tests [22], was close to that of pure water. Consequently, spherical micelles or short rodlike micelles that do not contribute to the viscosity of the solution are present at these conditions. Detecting rather long rodlike micelles in the P4VP-containing solution is suggested to be the result of the solubilization of polymer chains by the micelles. Furthermore, branches in the micellar solutions at such low concentration of surfactant have never been observed before. As was shown by computer modelling, solubilization of P4VP induced the formation of additional branching points in the hybrid micelles by attaching the energetically unfavorable end-caps to the polymer-loaded cylindrical fragments [26, 27].

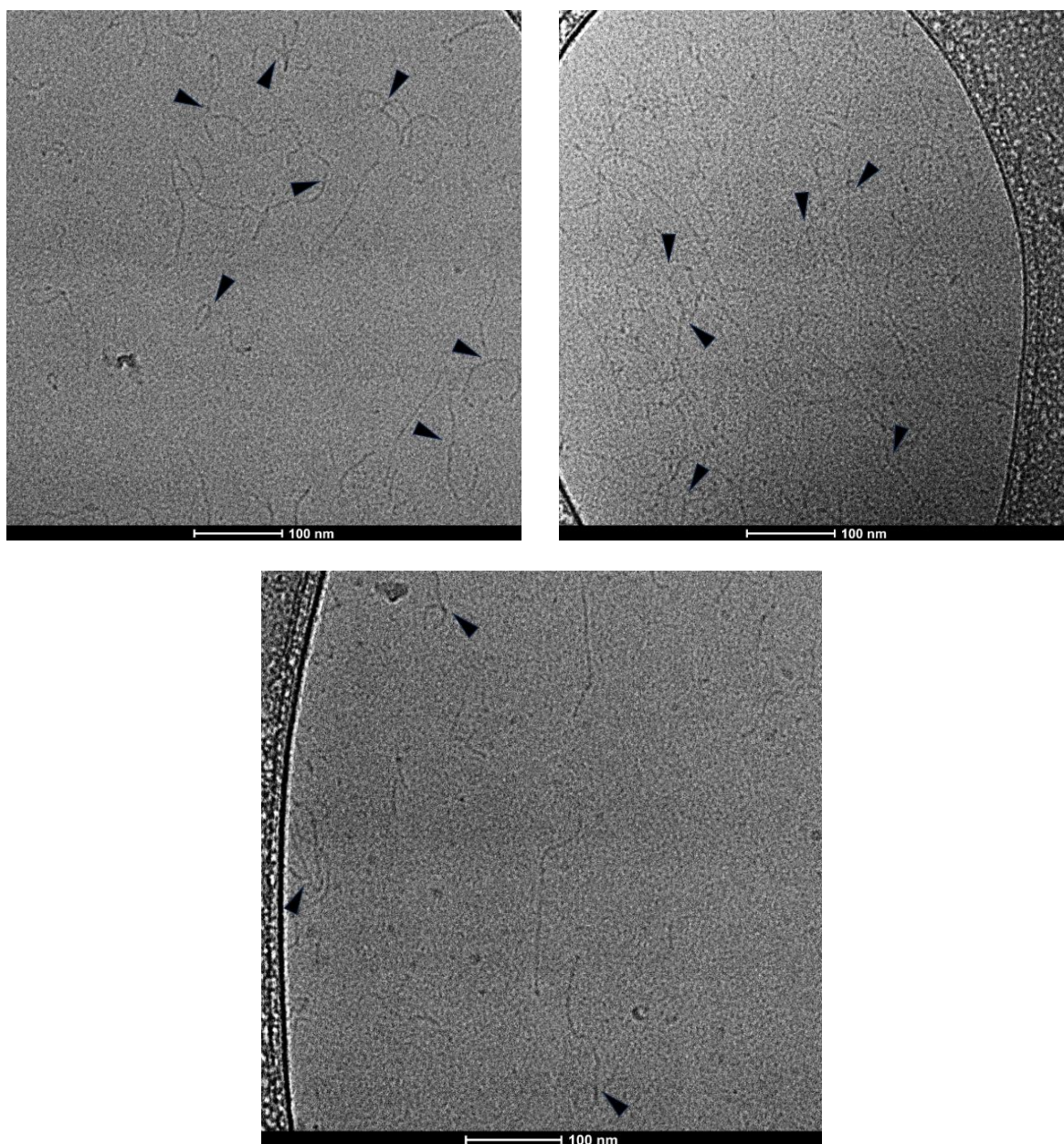


Figure 1. Spherical polymer-free micelles and prolate hybrid micelles in aqueous solution of 12.5 mM potassium oleate and 80 mM KCl, containing $2 \cdot 10^{-3}$ monomol/L P4VP, as imaged with cryo-TEM. The arrows point out the branching points in the hybrid micelles

The shape of hybrid micelles with different amount of embedded P4VP was revealed by SANS using contrast variation technique. In Figure 2a the neutron scattering intensity in the range of the small values of scattering vector Q behaves as: $I \sim Q^{-1}$. The scattering intensity $I(Q)$ from the rodlike particles can be expressed as [28]:

$$I(Q) = \Delta\rho^2 V_0 Q^{-1} \exp\left(-\frac{R^2 Q^2}{2}\right), \quad (1)$$

where $\Delta\rho = \rho_{OK} - \rho_{solvent}$ is the scattering contrast, equal to the difference between the scattering density of potassium oleate and of the solvent, V_0 and R are the volume and radius of the rods. Consequently, in the case of rodlike scatterers, $\ln(IQ)$ vs Q^2 dependence should represent a straight line with the slope $a = -0.5 \cdot R^2$. Therefore, Q^{-1} -scaling in low- Q region of the scattering curves (Fig. 2a) indicates the local cylindrical shape of the hybrid micelles at all studied concentrations of P4VP. The linear behavior of the corresponding $\ln(IQ)$ vs Q^2 dependencies confirms this observation (Fig. 2b). Mean radius of the hybrid micelles, estimated from the slopes of the dependencies, circa equals to 2 nm for all studied solutions and corresponds to one, evaluated from cryo-TEM image (Fig. 1).

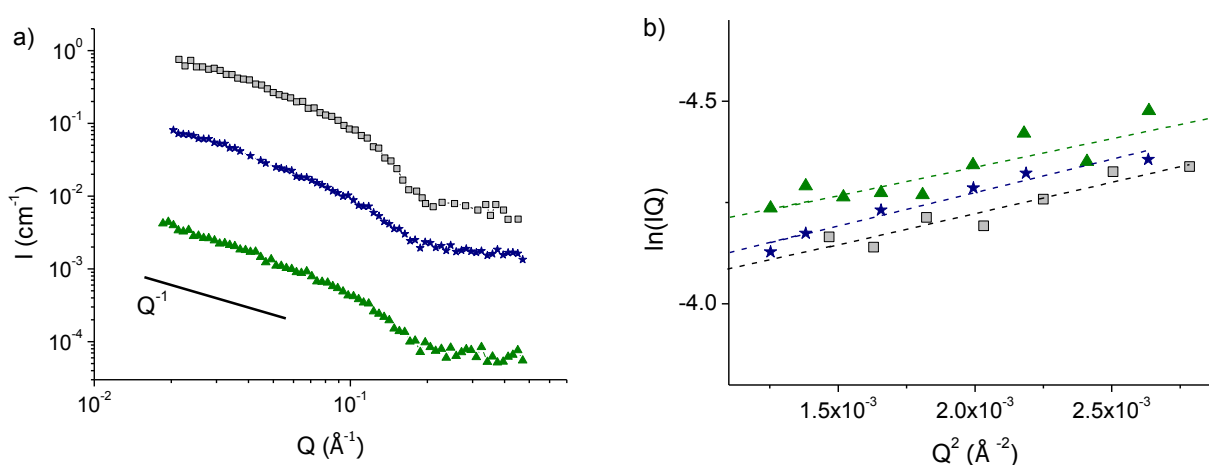


Figure 2. SANS curves in $I(Q)$ (a) and $\ln(IQ)$ vs Q^2 (b) representations for micellar solutions of 47 mM potassium oleate with different concentrations of embedded P4VP: 0.01 monomol/L (squares); 0.02 monomol/L (stars); 0.03 monomol/L (triangles). Matching the scattering from P4VP is used (solvent: 80 mM KCl in $D_2O/H_2O=37/73$ (v/v), pH=11). The data for solutions with 0.01 monomol/L P4VP are actual values, data for solutions containing 0.02 monomol/L and 0.03 monomol/L are shifted by a factor of 10 and 100 for clarity. The solid line shows the slope of the $I \sim Q^{-1}$ dependence. The dashed lines are linear fits of the dependences

The relaxation processes in aqueous solutions of hybrid micelles were studied by DLS. The autocorrelation functions $g^{(1)}(q, t)$ of the scattered visible light by hybrid micelles with different amount of embedded P4VP decay multi-exponentially (Fig. 3a). Thus, in the corresponding decay time distributions $A(t)$ three relaxation modes with relaxation rates Γ_1 , Γ_2 and Γ_3 can be observed (Fig. 3b). The obtained DLS data are very close to those of semi-dilute solutions of the entangled polymer chains and WLMs [29–31]. Therefore, in the case of hybrid WLMs the fast (I) and medium (II) relaxation modes (Fig. 2b), like in semi-dilute solutions of WLMs, could be attributed to translational diffusion of the chain segments and to the hindered motion of the entangled chains, respectively. Linear shape of the dependencies of the relaxation rates Γ_1 and Γ_2 on q^2 for fast and medium processes (Fig. 4a and b, respectively) confirm that they represent diffusive motion. By contrast, a non-linear dependence for slow (III) relaxation mode (Fig. 4c) suggests that this mode is the non-diffusive one. It is, probably, related to electrostatic repulsion of the similarly charged hybrid micelles of potassium oleate.

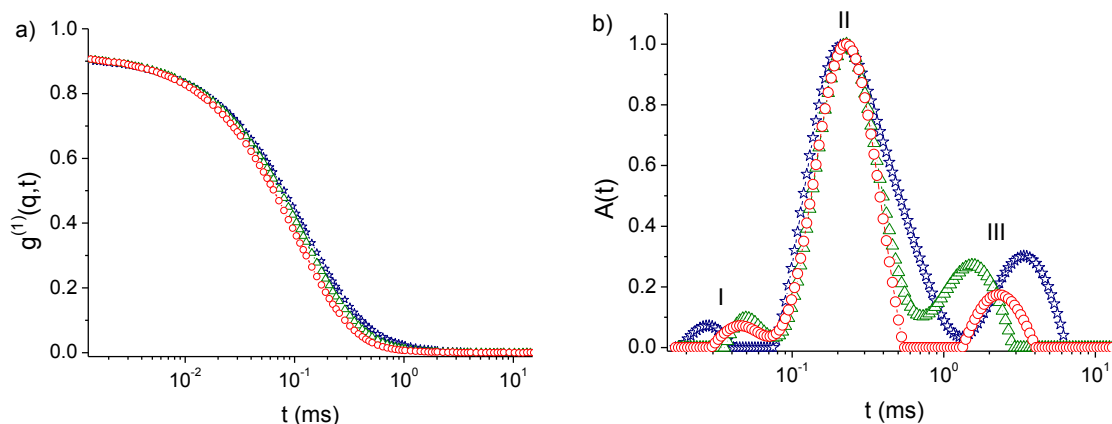


Figure 3. Field autocorrelation functions $g^{(1)}(q, t)$ (a) and decay time distributions $A(t)$ (b) at scattering angle $\theta=90^\circ$ for micellar solutions of 47 mM potassium oleate with different concentrations of embedded P4VP: 0.02 monomol/L (stars); 0.03 monomol/L (triangles) and 0.04 monomol/L (circles). Solvent: 80 mM KCl in water at pH=11

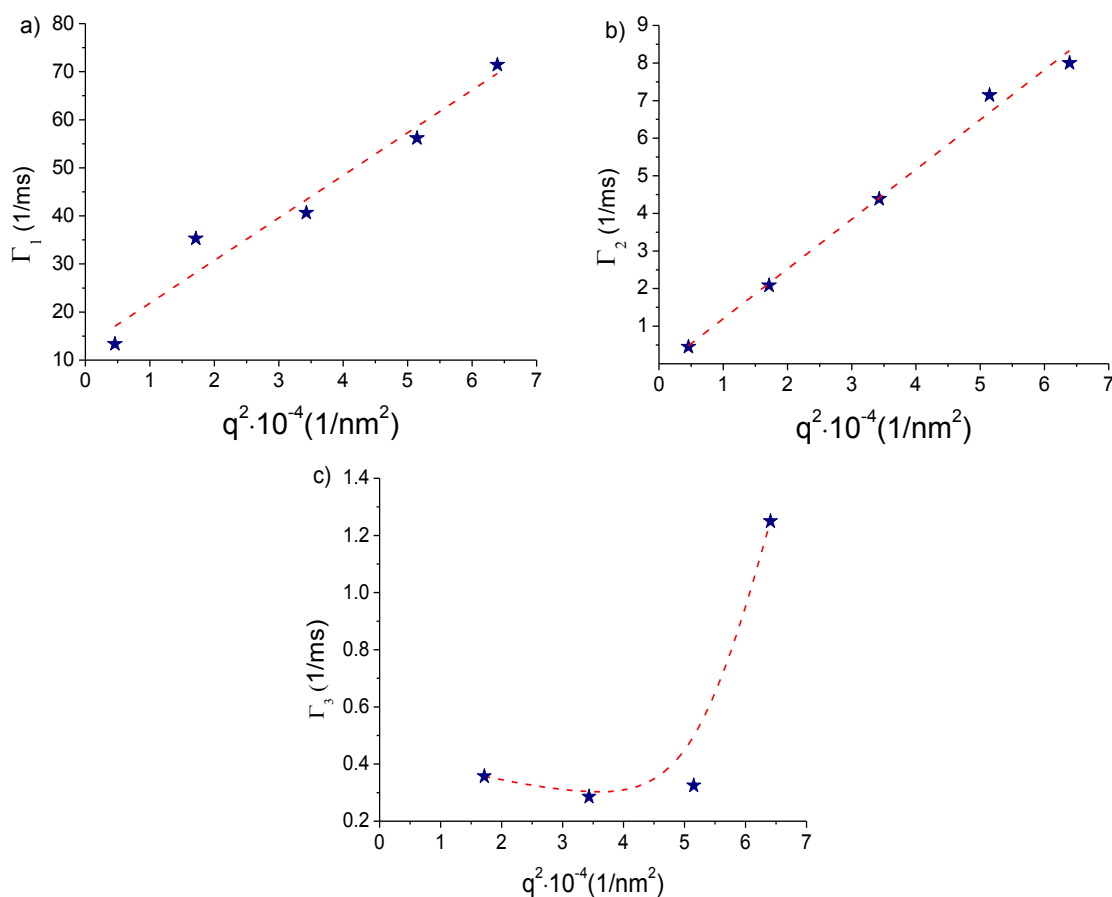


Figure 4. Γ vs q^2 dependences for first (a), second (b) and third (c) components of the field autocorrelation function $g^{(1)}(q, t)$ of the hybrid micelles in 47 mM solution of potassium oleate containing 0.02 monomol/L of P4VP. Solvent: 80 mM KCl in water at pH=11

Conclusions

Cryo-TEM, DLS and SANS were applied to shed light on the shape of hybrid micelles in the aqueous solutions of anionic surfactant potassium oleate with embedded hydrophobic polymer P4VP. Cryo-TEM evidenced the presence of branched rodlike micelles with mean length of 200 nm that is close to the averaged contour length of solubilized P4VP chains. Formation of branches in the hybrid micelles was caused by attaching of the thermodynamically unfavorable end-caps of micelles to the polymer-loaded central cylindrical

parts. The local cylindrical shape of hybrid micelles, as was shown by SANS, was independent of the concentration of solubilized P4VP. Values of radii of the micelles, estimated from cryo-TEM- and SANS data were equal to the length of hydrophobic “tail” of potassium oleate. Relaxation processes in the hybrid micelles were shown by DLS to be quite similar to those in polymer-free WLMs of surfactant: two relaxation modes were attributed to diffusion of the entangled micellar chains and their segments; the third mode was related to the electrostatic repulsion between similarly charged micelles.

Funding

This research was financially supported by the Russian Science Foundation (project № 21-73-10197).

Author Information*

**The authors' names are presented in the following order: First Name, Middle Name and Last Name*

Alexander Lvovich Kwiatkowski (*corresponding author*) — Candidate of physical and mathematical sciences, Leading Researcher, Lomonosov Moscow State University, Leninskie Gory, 1, 2, Moscow, 119991, Russia; e-mail: kviatkovskij@physics.msu.ru; <https://orcid.org/0000-0002-0514-384X>

Vyacheslav Sergeevich Molchanov — Candidate of physical and mathematical sciences, Docent, Lomonosov Moscow State University, Leninskie Gory, 1, 2, Moscow, 119991, Russia; e-mail: molchanov@polly.phys.msu.ru; <https://orcid.org/0000-0002-2846-0784>

Anton Sergeevich Orekhov — Candidate of physical and mathematical sciences, Researcher, National Research Center, Kurchatov Institute, pl. Academica Kurchatova, 1, Moscow, 123182, Russia; e-mail: orekhov.anton@gmail.com; <https://orcid.org/0000-0002-3006-2152>

Alexander Ivanovich Kuklin — Candidate of physical and mathematical sciences, Professor, Joint Institute of Nuclear Research, ul. Joliot-Curie, 6, Dubna, 141980, Russia; e-mail: alexander.iw.kuklin@gmail.com; <https://orcid.org/0000-0002-4530-2980>

Olga Evgenievna Philippova — Doctor of physical and mathematical sciences, Professor, Lomonosov Moscow State University, Leninskie Gory, 1, 2, Moscow, 119991, Russia; e-mail: phil@polly.phys.msu.ru; <https://orcid.org/0000-0002-1098-0255>

Author Contributions

The manuscript was written through contributions of all authors. All authors have given approval to the final version of the manuscript. **CRedit**: **Alexander Lvovich Kwiatkowski** investigation, original draft preparation, review and editing; **Vyacheslav Sergeevich Molchanov** investigation, conceptualization; **Anton Sergeevich Orekhov** investigation; **Alexander Ivanovich Kuklin** investigation; **Olga Evgenievna Philippova** original draft preparation, review and editing.

Conflicts of Interest

The authors declare no conflict of interest.

References

- Zana, R. (2005). Dynamics of Surfactant Self-Assemblies: Micelles, Microemulsions, Vesicles and Lyotropic Phases. Taylor and Francis Group. <https://doi.org/10.1081/DIS-200067928>
- Israelachvili, J. N., Mitchell, D. J., & Ninham, B. W. (1976). Theory of Self-Assembly of Hydrocarbon Amphiphiles into Micelles and Bilayers. *Journal of the Chemical Society, Faraday Transactions*, 72, 1525–1568. <https://doi.org/10.1039/f29767201525>
- Feng, Y., Chu, Z., & Dreiss, C. A. (2015). Smart Wormlike Micelles: Design, Characteristics and Applications. Springer-Verlag: Berlin, Heidelberg.
- Vlachy, N., Renoncourt, A., Drechsler, M., Verbavatz, J. M., Touraud, D., & Kunz, W. (2008). Blastulae aggregates: New intermediate structures in the micelle-to-vesicle transition of catanionic systems. *Journal of Colloid and Interface Science*, 320(1), 360–363. <https://doi.org/10.1016/j.jcis.2007.12.034>
- Israelachvili, J. N. (2011). Intermolecular and Surface Forces (3rd Ed). Academic Press.
- Zana, R., & Kaler, E. W. (2007). Giant Micelles: Properties and Applications. CRC Press.
- Chu, Z., Dreiss, C. A., & Feng, Y. (2013). Smart Wormlike Micelles. *Chemical Society Reviews*, 42(17), 7174–7203. <https://doi.org/10.1039/c3cs35490c>

- 8 Kwiatkowski, A. L., Molchanov, V. S., & Philippova, O. E. (2019). Polymer-like Wormlike Micelles of Ionic Surfactants: Structure and Rheological Properties. *Polymer Science — Series A*, 61(2), 215–225. <https://doi.org/10.1134/S0965545X19020081>
- 9 Falbe, J. (1987). Surfactants in Consumer Products: Theory, Technology and Application. In *Surfactants in Consumer Products: Theory, Technology and Application*. Springer-Verlag: Berlin, Heidelberg. <https://doi.org/10.1007/978-3-642-71545-7>
- 10 Ezrahi, S., Tuval, E., & Aserin, A. (2006). Properties, main applications and perspectives of worm micelles. *Advances in Colloid and Interface Science*, 128–130(2006), 77–102. <https://doi.org/10.1016/j.cis.2006.11.017>
- 11 Rodrigues, R. K., Folsta, M. G., Martins, A. L., & Sabadini, E. (2016). Tailoring of wormlike micelles as hydrodynamic drag reducers for gravel-pack in oil field operations. *Journal of Petroleum Science and Engineering*, 146, 142–148. <https://doi.org/10.1016/j.petrol.2016.04.021>
- 12 Le Garrec, D., Ranger, M., & Leroux, J. C. (2004). Micelles in anticancer drug delivery. *American Journal of Drug Delivery*, 2(1), 15–42. <https://doi.org/10.2165/00137696-200402010-00002>
- 13 Kim, J. H., Domach, M. M., & Tilton, R. D. (1999). Pyrene micropartitioning and solubilization by sodium dodecyl sulfate complexes with poly(ethylene glycol). *Journal of Physical Chemistry B*, 103(48), 10582–10590. <https://doi.org/10.1021/jp991720z>
- 14 Kuntz, D. M., & Walker, L. M. (2007). Solution Behavior of Rod-Like Polyelectrolyte-Surfactant Aggregates Polymerized from Wormlike Micelles. *Journal of Physical Chemistry B*, 111(23), 6417–6424. <https://doi.org/10.1021/jp0688308>
- 15 Massiera, G., Ramos, L., & Ligoure, C. (2002). Hairy Wormlike Micelles: Structure and Interactions. *Langmuir*, 18(15), 5687–5694. <https://doi.org/10.1021/la025687a>
- 16 Nakamura, K., & Shikata, T. (2007). Small Angle Neutron Scattering Study of Polyelectrolyte Conformation Incorporated Into Hybrid Threadlike Micelles Under Strong Shear Flows. *Journal of Physical Chemistry B*, 111(43), 12411–12417. <https://doi.org/10.1021/jp072975c>
- 17 Oikonomou, E., Bokiias, G., Kallitsis, J. K., & Iliopoulos, I. (2011). Formation of Hybrid Wormlike Micelles upon Mixing Cetyl trimethylammonium Bromide with Poly(methyl Methacrylate-co-Sodium Styrene Sulfonate) Copolymers in Aqueous Solution. *Langmuir*, 27(8), 5054–5061. <https://doi.org/10.1021/la200017j>
- 18 Myhre, S., Amann, M., Willner, L., Knudsen, K. D., & Lund, R. (2020). How Detergents Dissolve Polymeric Micelles: Kinetic Pathways of Hybrid Micelle Formation in SDS and Block Copolymer Mixtures. *Langmuir*, 36(43), 12887–12899. <https://doi.org/10.1021/acs.langmuir.0c02123>
- 19 Khannanov, A., Rossova, A., Ulakhovich, N., Evtugyn, V., Valiullin, L., Nabatov, A., Kutyrev, G., & Kutyreva, M. (2022). Doxorubicin-Loaded Hybrid Micelles Based on Carboxyl-Terminated Hyperbranched Polyester Polyol. *ACS Applied Polymer Materials*, 4(4), 2553–2561. <https://doi.org/10.1021/acsapm.1c01863>
- 20 Kwiatkowski, A. L., Molchanov, V. S., Kuklin, A. I., Orekhov, A. S., Arkharova, N. A., & Philippova, O. E. (2022). Structural transformations of charged spherical surfactant micelles upon solubilization of water-insoluble polymer chains in salt-free aqueous solutions. *Journal of Molecular Liquids*, 347. <https://doi.org/10.1016/j.molliq.2021.118326>
- 21 Kwiatkowski, A. L., Molchanov, V. S., Chesnokov, Y. M., Ivankov, O. I., & Philippova, O. E. (2023). Hybrid Polymer-Surfactant Wormlike Micelles for Concurrent Use for Oil Recovery and Drag Reduction. *Polymers*, 15(23). <https://doi.org/10.3390/polym15234615>
- 22 Molchanov, V. S., Philippova, O. E., Khokhlov, A. R., Kovalev, Y. A., & Kuklin, A. I. (2007). Self-assembled networks highly responsive to hydrocarbons. *Langmuir*, 23(1), 105–111. <https://doi.org/10.1021/la061612l>
- 23 Iancu, C. V., Tivol, W. F., Schooler, J. B., Dias, D. P., Henderson, G. P., Murphy, G. E., Wright, E. R., Li, Z., Yu, Z., Briegel, A., Gan, L., He, Y., & Jensen, G. J. (2007). Electron cryotomography sample preparation using the vitrobot. *Nature Protocols*, 1(6), 2813–2819. <https://doi.org/10.1038/nprot.2006.432>
- 24 Kuklin, A. I., Soloviov, D. V., Rogachev, A. V., Utrobin, P. K., Kovalev, Y. S., Balasoiu, M., Ivankov, O. I., Sirotin, A. P., Murugova, T. N., Petukhova, T. B., Gorshkova, Y. E., Erhan, R. V., Kutuzov, S. A., Soloviev, A. G., & Gordeliy, V. I. (2011). New opportunities provided by modernized small-angle neutron scattering two-detector system instrument (YuMO). *Journal of Physics: Conference Series*, 291(1), 1–7. <https://doi.org/10.1088/1742-6596/291/1/012013>
- 25 Hassan, P. A., Rana, S., & Verma, G. (2015). Making sense of brownian motion: Colloid characterization by dynamic light scattering. *Langmuir*, 31(1), 3–12. <https://doi.org/10.1021/la501789z>
- 26 Kwiatkowski, A. L., Sharma, H., Molchanov, V. S., Orekhov, A. S., Vasiliev, A. L., Dormidontova, E. E., & Philippova, O. E. (2017). Wormlike surfactant micelles with embedded polymer chains. *Macromolecules*, 50(18), 7299–7308. <https://doi.org/10.1021/acs.macromol.7b01500>
- 27 Kwiatkowski, A. L., Molchanov, V. S., Kuklin, A. I., & Philippova, O. E. (2020). Opposite effect of salt on branched wormlike surfactant micelles with and without embedded polymer. *Journal of Molecular Liquids*, 311, 113301–113309. <https://doi.org/10.1016/j.molliq.2020.113301>
- 28 Svergun, D., & Feigin, L. (1987). *Structure Analysis by SANS and SAXS*. Plenum Press.
- 29 Calabrese, M. A., & Wagner, N. J. (2018). Detecting Branching in Wormlike Micelles via Dynamic Scattering Methods. *ACS Macro Letters*, 7(6), 614–618. <https://doi.org/10.1021/acsmacrolett.8b00188>
- 30 Li, J., Ngai, T., & Wu, C. (2010). The slow relaxation mode: From solutions to gel networks. *Polymer Journal*, 42(8), 609–625. <https://doi.org/10.1038/pj.2010.59>
- 31 Wu, C., & Ngai, T. (2004). Reexamination of slow relaxation of polymer chains in sol-gel transition. *Polymer*, 45(6), 1739–1742. <https://doi.org/10.1016/j.polymer.2003.11.045>